Additional File for "Cell-nanoparticle stickiness and dose delivery in a multi-model *in silico* platform: DosiGUI"

Ermes Botte[a,b], Pietro Vagaggini[a], Ilaria Zanoni[c], Nicole Guazzelli[a], Lara Faccani[c], Davide Gardini[c], Anna L. Costa[c] and Arti Ahluwalia[a,b,]*

[a]Research Centre "E. Piaggio", University of Pisa, Pisa, Italy

[b]Department of Information Engineering, University of Pisa, Pisa, Italy

[c]CNR-ISSMC, National Research Council of Italy, Institute of Science, Technology and Sustainability for Ceramics, Faenza, Italy

*corresponding author: Arti Ahluwalia, Research Centre "E. Piaggio" – University of Pisa, Largo Lucio Lazzarino 1, 56125 Pisa, Italy, +39 0502217062; e-mail: arti.ahluwalia@unipi.it.

AF1 – A practical guide for downloading, installing and running DosiGUI

DosiGUI was developed as an open source, standalone desktop application using the MATLAB computing environment (R2022b). Its source code was compiled to run as a desktop application for both Windows and iOS operating systems, without MATLAB.

The installer of the standalone version of DosiGUI is freely available at this link. Before beginning the installation procedure, ensure you have a stable internet connection; then, follow the steps illustrated below.

1) Download the files attached at the link, by clicking on the green button *Code* and choosing "Download ZIP".

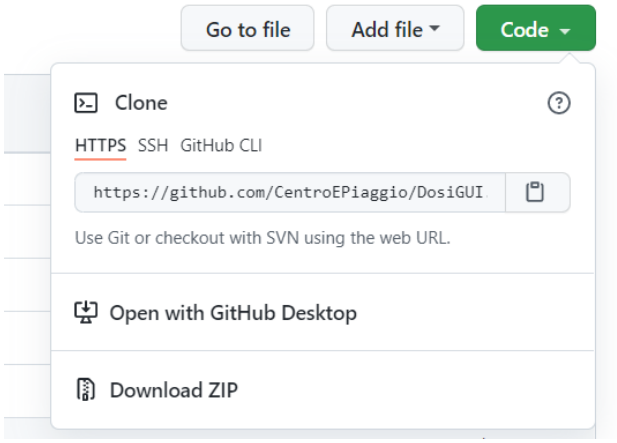

2) Unpack the executable file (*DosiGUI_Web_Installer*) suitable for your operating system. It is the installer of all required components for running DosiGUI as a desktop application. For Mac-users, please refer to the file *MacOS Readme.pdf* for further details, available at the same link in the folder "MacOS".
3) Launch the *DosiGUI_Web_Installer* executable file and wait for the loading window to appear.

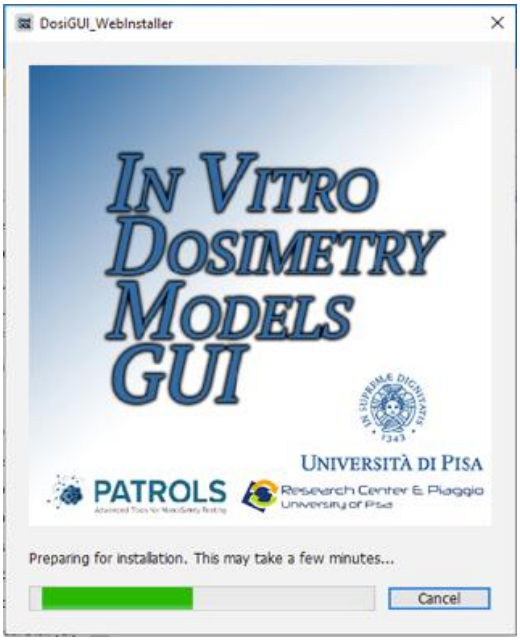

4) Once the loading is complete, a new window appears, where you can check the version of the application you are about to install. Click *Next* to proceed.

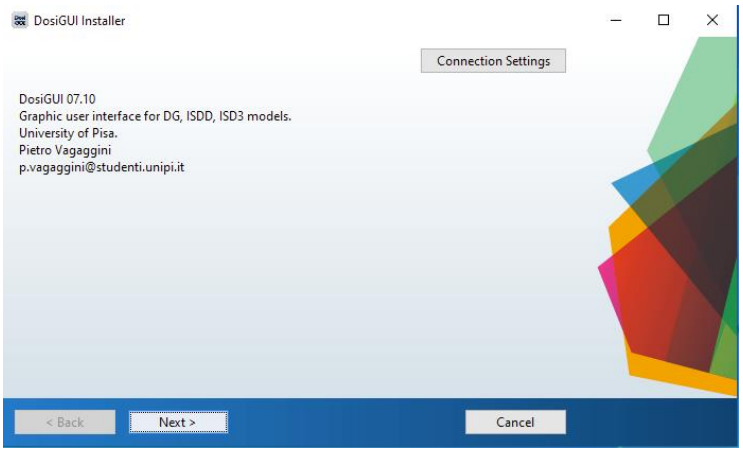

5) Choose the desired folder to install the application. It is recommended to keep the default settings and check the option “Add a shortcut to the desktop”.

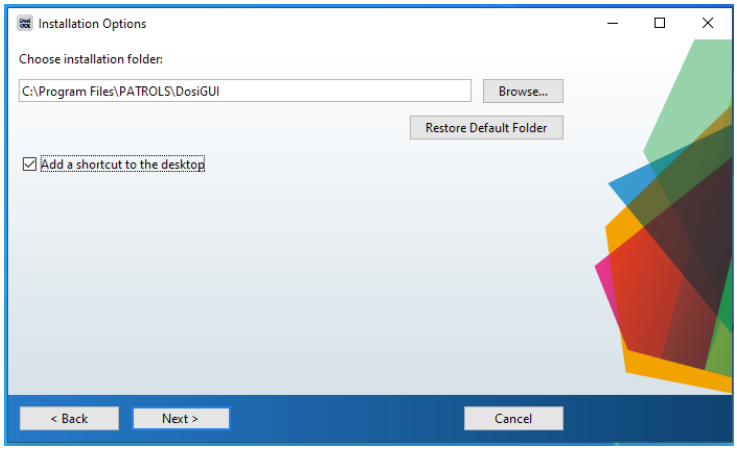

6) Choose the desired folder to install MATLAB Runtime (version 9.13, a free MATLAB component required to run DosiGUI). It is recommended to keep the default settings.

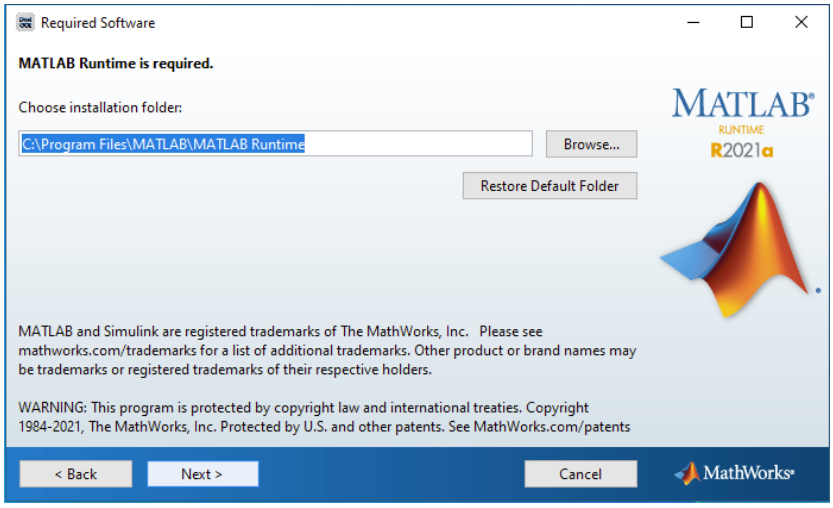

7) Accept the license agreement for MATLAB Runtime and click *Next*.

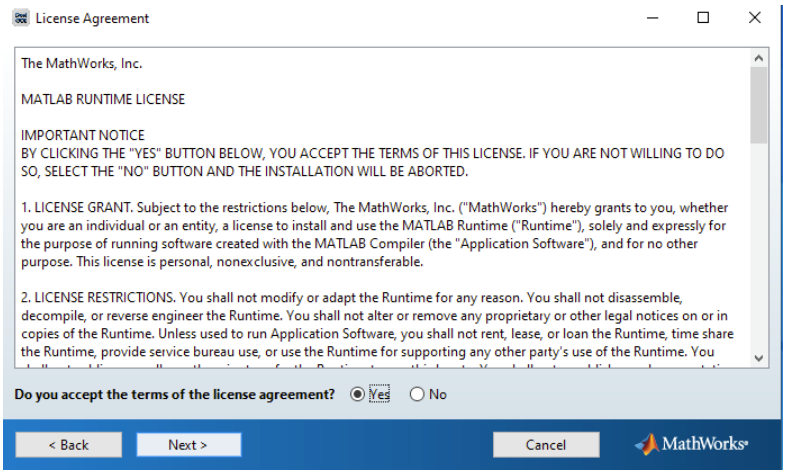

8) A confirmation window summarizing the installation settings appears. Click *Install* to start the installation.

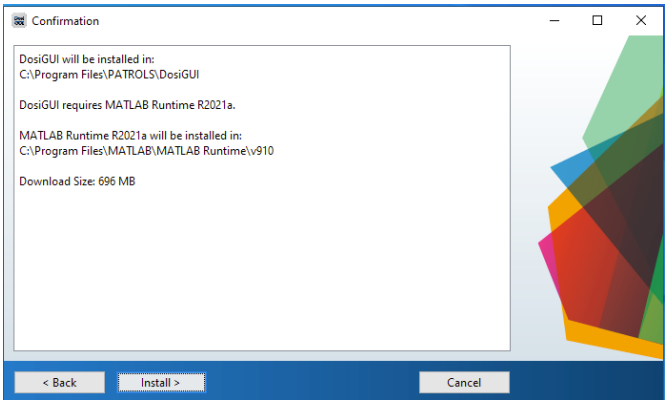

9) The operation begins with the download and installation of MATLAB Runtime (approximately 500MB). Then, DosiGUI is installed.

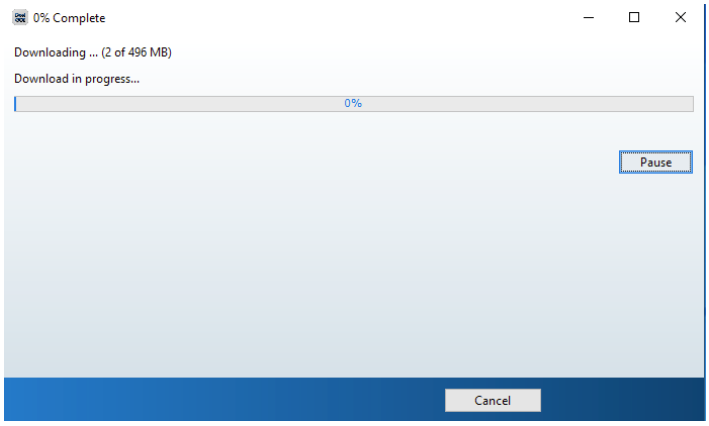

10) Once the installation is complete, close the installer window. Now, you should be able to run DosiGUI from the shortcut on your desktop.

Launching the application from the desktop shortcut opens a main window where a brief description of ISD3 and DG is provided (Figure A1A). After initiating one of the two models by clicking on the corresponding *Start* button, the user can manually enter all input parameters needed for running simulations. Alternatively, a pop-up menu (Figure A1B) allows the input parameters to be either directly loaded from a specific file containing the information requested for the chosen model (*Load from file*) or obtained by automatic rearrangement of an input file which may have been already stored for the other model (in Figure A1B, *Load DG simulation*). A single harmonized input dataset which is suitable for both models is one of the unique features of DosiGUI: the same experimental configuration can be simulated using ISD3 and

DG models, and the consistency of their predictions can be compared to determine the most suitable model for estimating the delivered dose of NPs for a given setup. As an example, Figure A1B shows the interface panels for the ISD3 model and all categories of inputs it requires, including intrinsic and extrinsic parameters (left side). Specific plot settings are also listed on the right: predicted delivered doses as well as any other available output variable can be plotted as a function of time or height, and the generated figures can be saved as .png, .jpg, .tif or .pdf files. Once started, a status bar shows the current status of the simulation. When the simulation is complete, inputs and outputs are saved as .xlsx and .mat files. Finally, all calculations performed by DosiGUI are summarized and saved into a .txt file named *logfile*. The logfile helps in identifying interruptions caused by computational errors when the GUI is running.

AF2 – DG and ISD3: analytical summary

Both the ISD3 and DG models refer to the dynamics of NPs suspended in a cylinder containing protein-enriched culture medium which a cell monolayer on the bottom is exposed to [1,2]. Considering a homogeneously sticky bottom boundary (*i.e.*, a homogeneously distributed cell monolayer), requirements for Cartesian symmetry are verified, thus the system can be studied by means of a 1D model representing the axial direction (x) only. Along this axis, three physical phenomena are taken into account: diffusion, sedimentation, and, if applicable, dissolution, described by the following rate equations.

$$R_{diff}(d_p; x, t) = D_{diff}(d_p) \frac{\partial^2 N(d_p; x, t)}{\partial x^2} \quad \text{(A1)}$$

$$R_{sed}(d_p; x, t) = -v_{sed}(d_p) \frac{\partial N(d_p; x, t)}{\partial x} \quad \text{(A2)}$$

$$R_{diss}(d_p; x, t) = -\frac{\partial}{\partial d_p}\left(N(d_p; x, t)\frac{\partial d_p}{\partial t}\right) \quad \text{(A3)}$$

The variables and parameters introduced in Eq. (A1) – (A3) are listed below:

- x (m) is the spatial coordinate;
- t (s) is the temporal coordinate;
- d_p (m) denotes the NP effective diameter (*i.e.*, the diameter of the NP and its solution-dependent corona);
- R_{diff}, R_{sed} and R_{diss} (m^{-2} s^{-1}) are the diffusion, sedimentation and dissolution rates, respectively;
- N (m^{-2}) denotes the number surface density of NPs having a certain diameter d_p. N is the variable that the models solve for in each spatial point at each iteration and is defined for each NP size in the dispersion. Thus, the corresponding mass surface density field M (kg m^{-2}) is:

$$M(d_p; x, t) = \rho_{eff}\frac{\pi}{6}{d_p}^3 N(d_p; x, t) \quad \text{(A4)}$$

with ρ_{eff} (kg m^{-3}) the effective physical density of the NP (*i.e.*, the physical density of the protein-coated NP). Consequently, the nominal and delivered doses are given by Eq. (A5) and (A6), respectively.

$$M_{nom}(x) = M(x, 0) = \int M(d_p; x, 0)\partial d_p \quad \text{(A5)}$$

$$M_{del}(t) = M(0, t) = \int M(d_p; 0, t)\partial d_p \quad \text{(A6)}$$

- D_{diff} (m^2 s^{-1}) is the isotropic diffusion coefficient of each NP with diameter d_p, defined according to Eq. (A7) (Stokes-Einstein's equation):

$$D_{diff}(d_p) = \frac{RT}{3N_A \pi \mu d_p} \quad \text{(A7)}$$

with R (J mol^{-1} K^{-1}) the universal gas constant, T (K) the temperature of the suspension, N_A (mol^{-1}) the Avogadro's number and μ (Pa s) the dynamic viscosity of the culture medium;

- v_{sed} (m s^{-1}) is the steady-state sedimentation velocity of a NP of effective diameter d_p, which is given by Stokes' equation:

$$v_{sed}(d_p) = \frac{g(\rho_{eff} - \rho_f){d_p}^2}{18\mu} \quad \text{(A8)}$$

where g (m s^{-2}) is the gravitational acceleration and ρ_f (kg m^{-3}) is the density of the culture medium.

The dissolution rate (Eq. (A3)) can be simply treated as a constant, holding across all NP diameters. In the case of the DG model, which accounts for dissolution considering ${R_{diss}}^*$ (s^{-1}) – *i.e.*, the fraction of the initial number surface density of NPs with a specific diameter d_p dissolving per unit time – Eq. (A3) is a first order rate equation [1]:

$$R_{diss}(d_p; x) = -N(d_p; x, 0){R_{diss}}^* \quad \text{(A9)}$$

On the other hand, the ISD3 implements dissolution as a surface area-driven phenomenon based on a NP-specific kinetic model. This description can be more accurate but less general than that provided in Eq. (A9). It does however require an in-depth characterization of dissolution kinetics for determining an analytical formulation of the associated rate suitable for the NP of interest [2].

Combining the rate equations introduced so far results in a single PDE, which completely describes NP dynamics in protein-enriched aqueous media:

$$\frac{\partial N(d_p;x,t)}{\partial t} = D_{diff}(d_p)\frac{\partial^2 N(d_p;x,t)}{\partial x^2} - v_{sed}(d_p)\frac{\partial N(d_p;x,t)}{\partial x} - \frac{\partial}{\partial d_p}\left(N(d_p;x,t)\frac{\partial d_p}{\partial t}\right) \quad \text{(A10)}$$

Both models in DosiGUI solve the PDE in Eq. (A10) with respect to N for each existing NP size d_p, exploiting different numerical approaches [1,2].

AF3 – Boundary condition: further analytical details

The DG and ISD3 models represent the adsorption of NPs on the cell monolayer in different ways.

DG model

The DG model accounts for a sticky bottom by implementing a Langmuir adsorption kinetics (Eq. (1) in the main text). The instantaneous adsorption rate depends on the dissociation constant k_D, which is the parameter to be identified and set for modulating what we called stickiness [1]. In addition, note that the molar concentration $[NP](0,t)$ accounts for ENPs of all existing sizes d_p and can be immediately derived from the dependent variable of the model (*i.e.*, the number surface density of NPs, N) as:

$$[NP](0,t) = 10^{-3}\frac{\int N(d_p;0,t)\partial d_p}{N_A \Delta x} \quad \text{(A11)}$$

where Δx (m) is the spatial resolution of simulations (*i.e.*, the height of the simulation compartment) and the multiplying factor 10^{-3} is needed for converting from m^3 to L.

ISD3 model

ISD3 manages the characteristics of the bottom by means of a typical mixed boundary condition for the PDE in Eq. (A10) [2]. We have modified Thomas et al.'s equation describing

this boundary condition, by parametrizing it with respect to K (m), which determines the stickiness of the cell monolayer (Eq. (2) in the main text).

AF4 – Correlation analyses: statistical details

Correlation analysis was carried out for both model validation and identification of parameters modulating the cell-ENP stickiness. In particular, as shown in Figure A2, the regression line which best fits the trend of $\varphi_{h/2}^{exp}$ (or φ_a^{exp}) as a function of $\varphi_{h/2}^{sim}$ (or φ_a^{sim}) was determined with a confidence interval of 99% for each ENP and nominal dose. For improving its robustness, the fitting procedure was weighted according to the inverse of the squared standard deviation of each experimental measurement. DosiGUI predictions were considered as validated for the specific ENP (or the value of k_D or K giving the predictions considered was assumed as a suitable candidate for the specific ENP, cell type and nominal dose) on the basis of the following criteria:

- Pearson's coefficient $(r) \geq 0.5$ (*i.e.,* measurements and predictions are significantly correlated);
- $p \geq 0.01$ for the extra sum-of-squares F-test on the slope of the regression line, having the null hypothesis that the best-fit value of the parameter is not statistically distinguishable from 1 (*i.e.,* numerical values of predictions do not significantly differ from measurements).

Note that, since these are necessary but not sufficient conditions singularly, both criteria must be satisfied, starting for each nominal dose considered.

For stickiness parameter identification, the most suitable value of K or k_D was determined as that maximizing both the computed statistics (*i.e.,* the Pearson's coefficient r and the p-value p of the extra sum-of-squares F-test). If slightly different values were identified for the same

ENP starting from different nominal doses, the overall optimal value of K or k_D (K_{opt} or $k_{D,opt}$) for the ENP was defined as:

$$K_{opt} = \sum_i w_i K_i \quad \text{(A12)}$$

where i indices nominal doses, K_i (m) is the stickiness which optimizes correlation statistics for the i-th nominal dose, and $w_i = r_i p_i / \sum_i r_i p_i$ denotes the weighting for K_i depending on r and p of the associated regression line. For instance, Eq. (A12) reports the case of the ISD3 model; the same rationale held for the definition of $k_{D,opt}$ in the DG model.

AF5 – Sticky gel preparation

To mimic the typical thickness of a cell monolayer, firstly, 1% w/v of gelatin (Sigma-Aldrich®) was dispersed in MilliQ water and left stirring at 70 °C until complete dissolution (about 30 min). Then, 100 µL of GPTMS (Alfa Aesar®) per gram of gelatin were added for cross-linking, and the solution was again stirred for 30 min at 70 °C. Finally, the bottom of the vial was coated using 626 µL of the solution, letting it gel overnight at room temperature before conducting the exposure and mid-height sampling studies.

AF6 – Protocol for mid-height sampling of ENP suspensions

An experimental protocol internally validated in CNR-ISSMC laboratories was used to perform mid-height sampling. Briefly, we collected 3 mL samples from the middle of the suspension column with a 5 mL micropipette. The tip of the pipette was positioned at mid-height so as to collect the suspension from 3.00 cm down to 2.25 cm from the bottom of the vial (Figure A3). Samples were first processed by acid treatment, adding 0.3 mL of 65% v/v solution of nitric acid (HNO_3 - Sigma-Aldrich, St. Louis, MI, USA). Then, their elemental

composition – and hence the mid-height mass concentration of ENPs ($c_{h/2}$ in Eq. (3) of the main text) – was determined using an ICP-OES 5100 – vertical dual view apparatus coupled with OneNeb nebulizer (Agilent Technologies, Santa Clara, CA, USA). Calibration curves for such measurements were obtained via commercial standard solutions (Sigma-Aldrich - St. Louis, MI, USA – with ENP concentrations of 0.05, 0.10, 1.00, 10.00 and 100.00 μg/mL), preliminary treated with the digestive procedure described above.

AF7 - Cell culture protocols

HepG2, A549 and Caco-2 cells were cultured in T75 flasks (Sarstedt®, Numbrecht, Germany) with initial seeding densities as specified by the provider. They were supplied with 12 mL of fresh DMEM every 3 days and expanded until 90% confluence was reached. At this stage, the medium was fully removed, and the cells rinsed with 3 mL of PBS. 3 mL of trypsin-EDTA was then added and left incubating for 5 min (37 °C, 5% CO_2, 95% RH) for cell detachment. Finally, an equal volume of DMEM was used to inactivate trypsin-EDTA, and residually adherent cells were collected by gently pipetting the suspension. For each cell type, one third of the suspension was used to plate cells in a new flask. The remainder was used to generate confluent monolayers in 96-well plates.

A

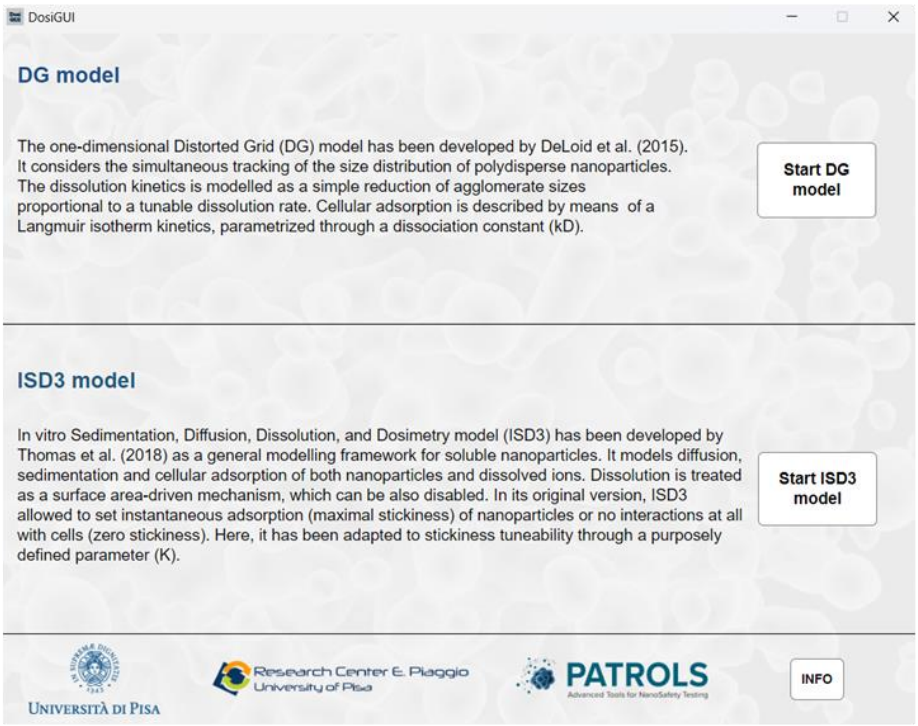

B

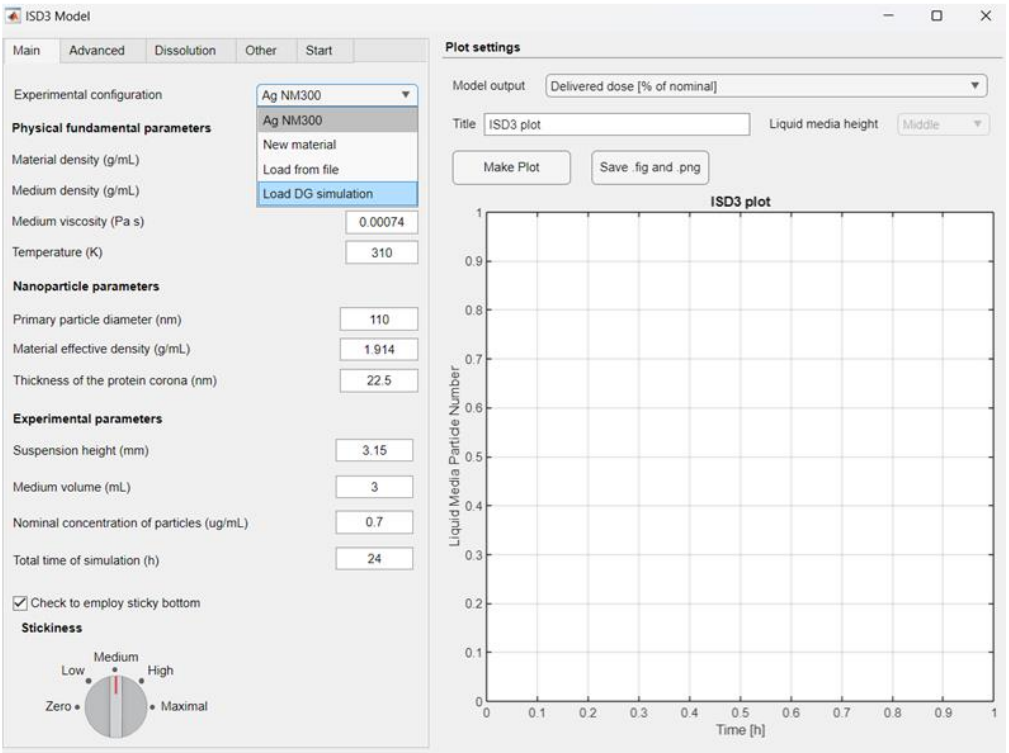

Figure A1. The graphical user interface. **A)** The main window of DosiGUI. **B)** The interface panel for the ISD3 model. The input values shown refer to the validation of ISD3 for silver (Ag - NM-300K) nano-dosimetry, carried out in ref [3].

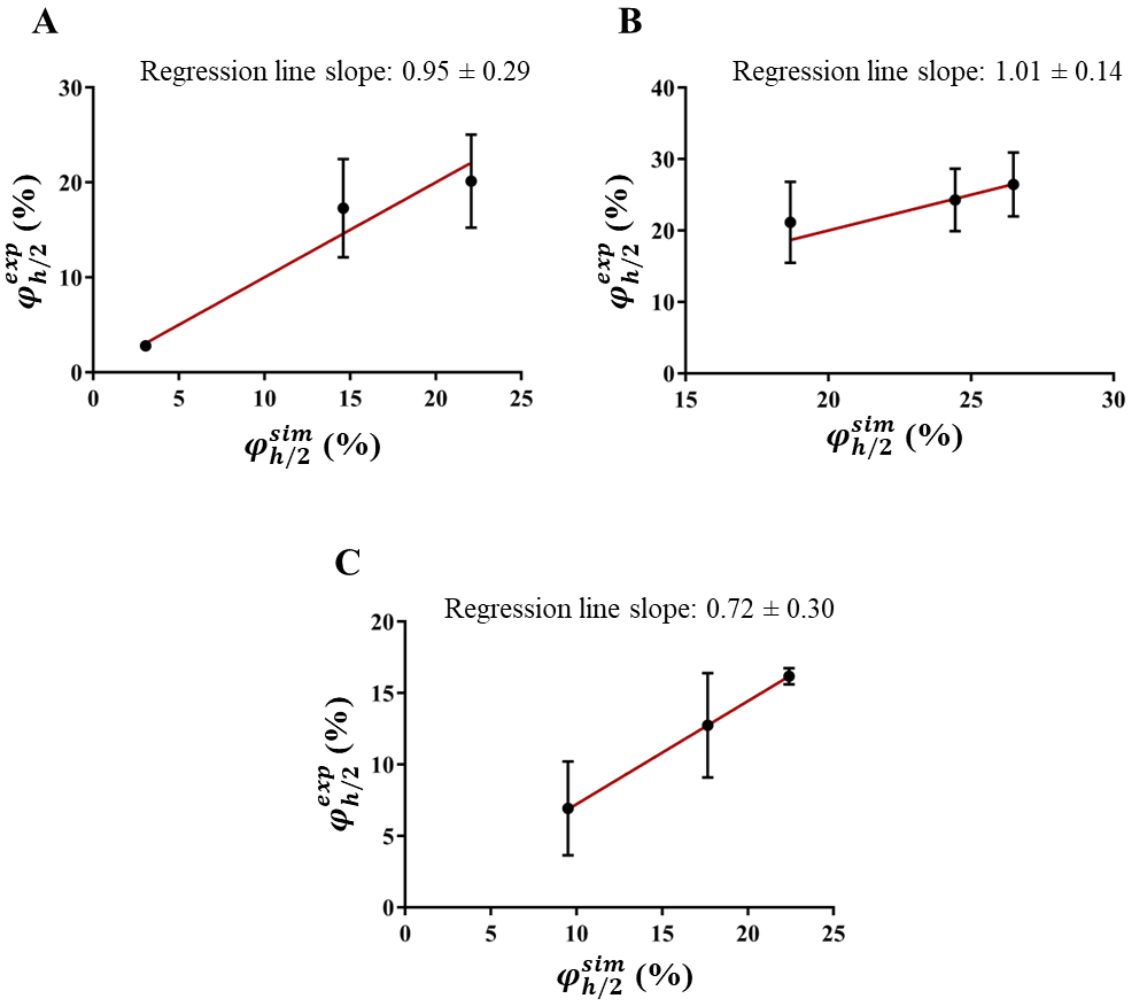

Figure A2. Examples of correlation fitting performed for validating DosiGUI predictions using the DG model (see Table 1 in the main text for associated correlation statistics). **A)** TiO_2 (NM-105), sticky bottom, M_{nom} = 125 µg cm^{-2}; **B)** CeO_2 (NM-212), sticky bottom, M_{nom} = 250 µg cm^{-2} and **C)** $BaSO_4$ (NM-220), reflective bottom, M_{nom} = 250 µg cm^{-2}. Experimental data are shown as mean ± standard deviation, while slopes of the best fitting regression line are reported as median values with a confidence interval of 99%.

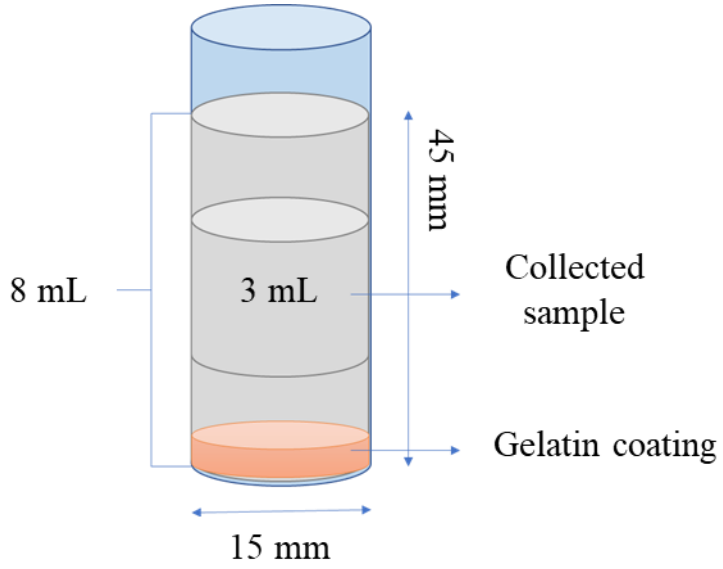

Figure A3. Experimental setup for mid-height sampling of ENP suspensions in the case of gelatin-coated (*i.e.*, maximally sticky) bottom.

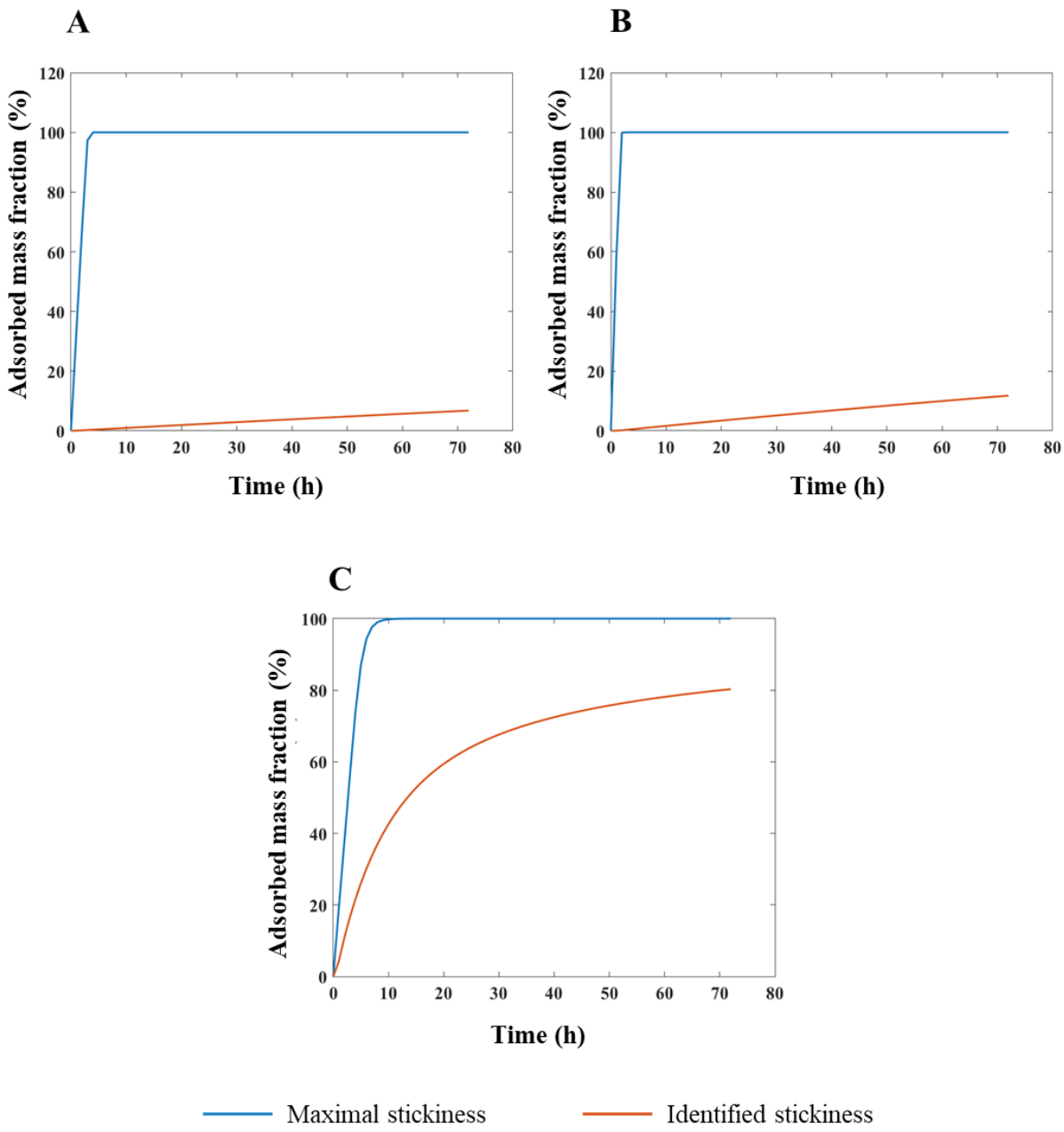

Figure A4. Predictions of mass fraction over time adsorbed by HepG2 cells expressed as a percentage of the total amount of ENP mass in the suspension, obtained running ISD3 within DosiGUI and assuming a nominally administered dose of 78.1 µg/cm^2. Comparison between the case of a maximally sticky bottom (blue line) and the identified stickiness of HepG2 monolayers (orange line) for: **A)** TiO_2 (NM-105), **B)** CeO_2 (NM-212) and **C)** $BaSO_4$ (NM-220). Note that, unlike the DG model, setting a maximal stickiness in the ISD3 model implies that the initially administered mass of each ENP is completely adsorbed on the bottom in few hours. This is because the DG model simulates surface occupancy and saturation, whereas ISD3 does not impose such surface condition and thus the boundary acts like a sink.

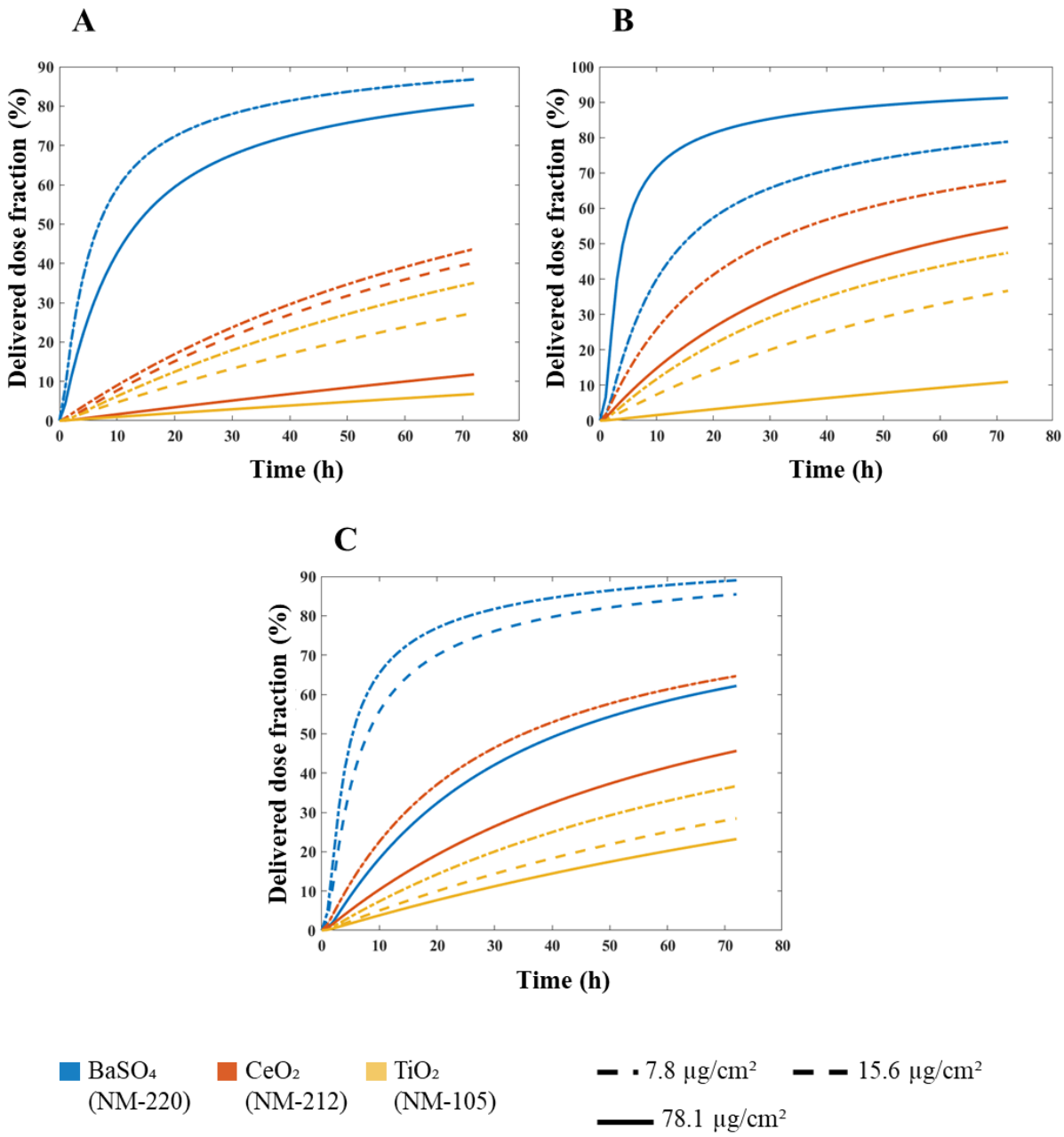

Figure A5. Predictions for the dose fraction (*i.e.*, delivered dose/nominal dose, percentage) versus exposure time obtained running the ISD3 model within DosiGUI, delivered to **A)** HepG2 cells, **B)** A549 cells and **C)** Caco-2 cells. Note that, for some ENP-cell type combinations, only two curves are visible because the delivered dose fraction profiles over time perfectly overlap starting from nominal doses of 7.8 and 15.6 µg cm^{-2}.

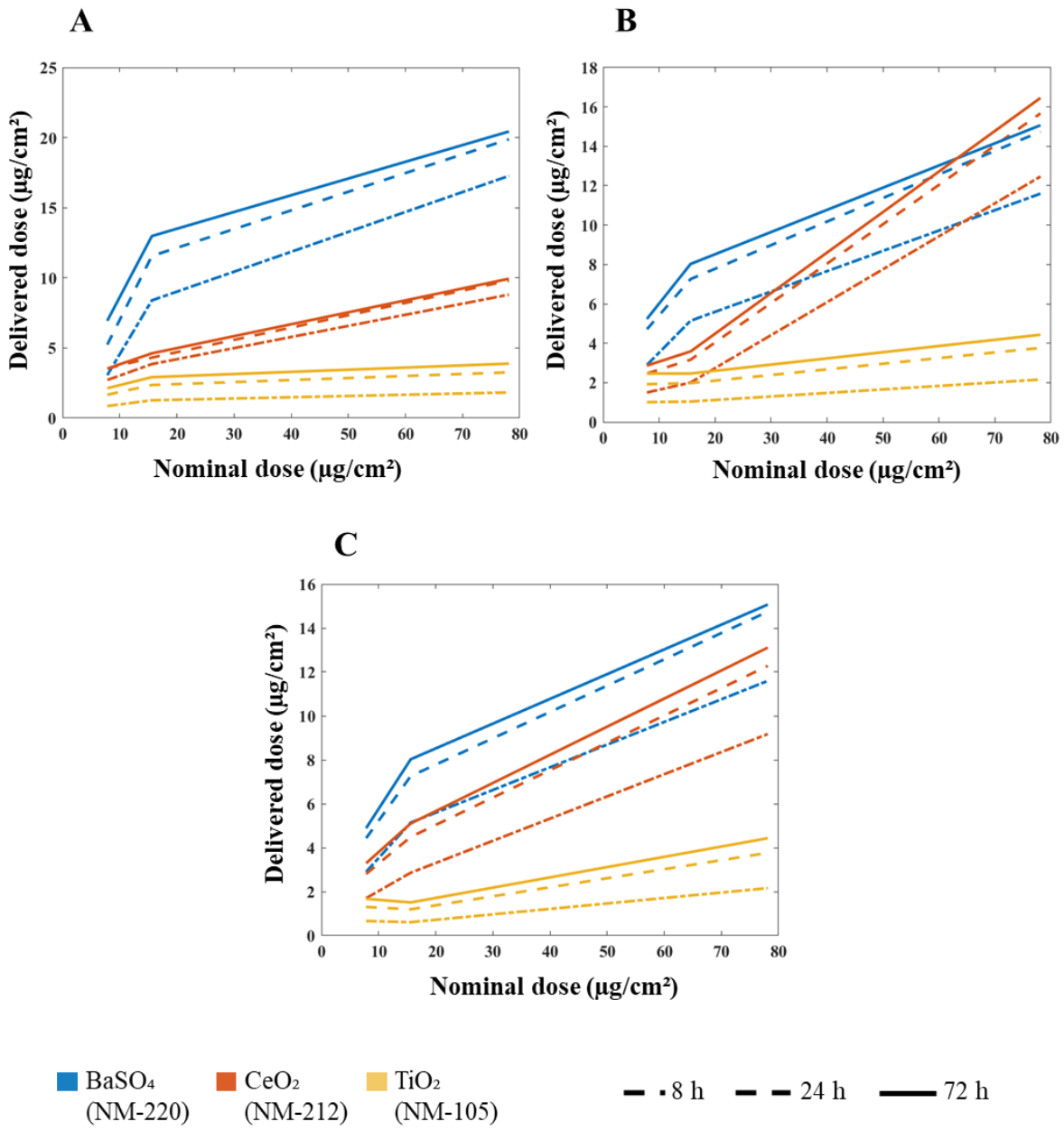

Figure A6. Predictions for the delivered dose versus nominal dose obtained running the DG model within DosiGUI, for **A)** HepG2 cells, **B)** A549 cells and **C)** Caco-2 cells.

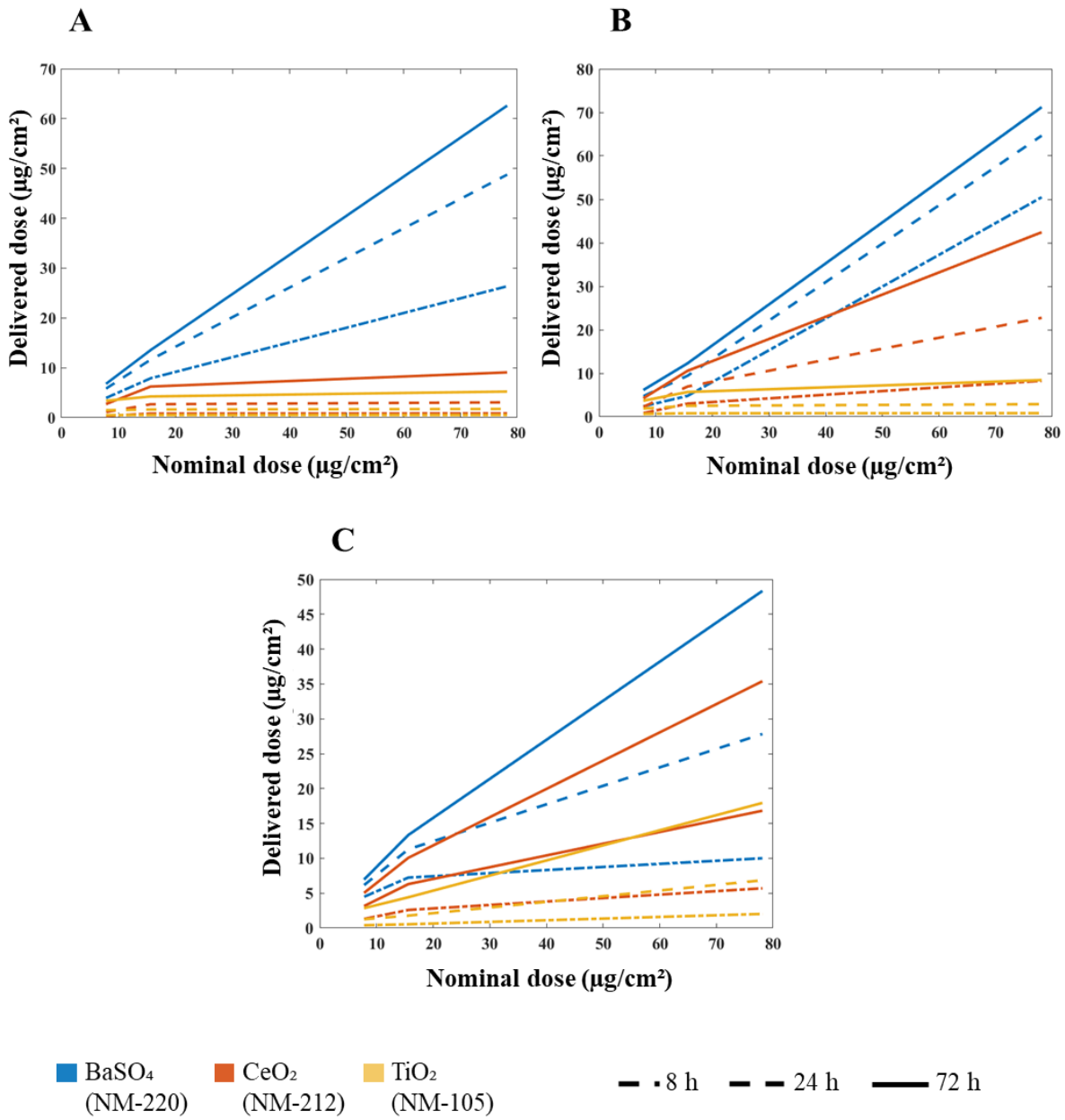

Figure A7. Predictions for the delivered dose versus nominal dose obtained running the ISD3 model within DosiGUI, for **A)** HepG2 cells, **B)** A549 cells and **C)** Caco-2 cells.

Table A1. Fundamental input parameters common to all simulations performed for this work. Physicochemical properties of ENPs and characteristics of the culture medium are from [4].

Parameter	Assigned value
Medium density (ρ_f)	0.9995 g mL^{-1}
Medium dynamic viscosity (μ)	0.81 mPa s
TiO_2 (NM-105) size distribution*	Log-normal Mean: 464.5 nm, Standard deviation: 2.6 nm
TiO_2 (NM-105) density (ρ)	4.23 g mL^{-1}
TiO_2 (NM-105) effective density (ρ_{eff})**	1.41 g mL^{-1}
CeO_2 (NM-212) size distribution*	Log-normal Mean: 243.3 nm, Standard deviation: 3.0 nm
CeO_2 (NM-212) density (ρ)	7.21 g mL^{-1}
CeO_2 (NM-212) effective density (ρ_{eff})**	2.21 g mL^{-1}
$BaSO_4$ (NM-220) size distribution*	Log-normal Mean: 111.9 nm, Standard deviation: 4.5 nm
$BaSO_4$ (NM-220) density (ρ)	4.49 g mL^{-1}
$BaSO_4$ (NM-220) effective density (ρ_{eff})**	2.03 g mL^{-1}

* Hydrodynamic size distributions of ENPs were measured by DLS on freshly prepared suspensions (as detailed in the main text, subsection *DosiGUI validation*). ** Effective density values from previous papers [4,6] measured by volumetric centrifugation method [5].

Table A2. Specific input parameters of simulations performed for model validation.

Parameter	Assigned value
Suspension height (h)	45 mm
Temperature (T)	37 °C
Nominal dose (M_{nom})	25, 125, 250 µg cm^{-2}
Bottom stickiness parameters	k_D = 0 mol L^{-1}, K = 0 m (totally sticky) k_D = 10^{-5} mol L^{-1}, K = 10^{12} m (purely reflective)
Total exposure time (τ)	24 h
Spatial resolution (Δx)	0.5 mm
Time resolution (Δt)	60 s
Dissolution constants	Dissolution disabled

Table A3. Specific input parameters of simulations performed for identifying parameters describing the stickiness in both DG and ISD3.

Parameter	Assigned value
Suspension height (h)	3.125 mm
Temperature (T)	37 °C
Nominal dose (M_{nom})	7.8, 15.6, 78.1 µg cm^{-2}
Stickiness parameters	k_D $\in$ [1×10^{-12}; 1×10^{-7}] mol L^{-1} K $\in$ [1×10^{3}; 1×10^{10}] m
Exposure time (τ)	72 h
Spatial resolution (Δx)	0.05 mm
Time resolution (Δt)	1 s
Dissolution constants	Dissolution disabled

AF references

1. DeLoid GM, Cohen JM, Pyrgiotakis G, Pirela S V., Pal A, Liu J, et al. Advanced computational modeling for in vitro nanomaterial dosimetry. Part Fibre Toxicol. 2015;12:1–20.

2. Thomas DG, Smith JN, Thrall BD, Baer DR, Jolley H, Munusamy P, et al. ISD3: A particokinetic model for predicting the combined effects of particle sedimentation, diffusion and dissolution on cellular dosimetry for in vitro systems. Part Fibre Toxicol. 2018;15:1–22.

3. Poli D, Mattei G, Ucciferri N, Ahluwalia A. An Integrated In Vitro–In Silico Approach for Silver Nanoparticle Dosimetry in Cell Cultures. Ann Biomed Eng. 2020;1–10.

4. Keller JG, Quevedo DF, Faccani L, Costa AL, Landsiedel R, Werle K, et al. Dosimetry in vitro – exploring the sensitivity of deposited dose predictions vs. affinity, polydispersity, freeze-thawing, and analytical methods. Nanotoxicology. 2020;15:21–34.

5. DeLoid G, Cohen JM, Darrah T, Derk R, Rojanasakul L, Pyrgiotakis G, et al. Estimating the effective density of engineered nanomaterials for in vitro dosimetry. Nat Commun 2014 51. 2014;5:1–10.

6. Llewellyn S V., Conway GE, Zanoni I, Jørgensen AK, Shah U-K, Seleci DA, et al. Understanding the impact of more realistic low-dose, prolonged engineered nanomaterial exposure on genotoxicity using 3D models of the human liver. J Nanobiotechnology 2021 191. 2021;19:1–24.